American Mineralogist, Volume 90, pages 645–652, 2005

Anomalous elastic behavior and high-pressure structural evolution of zeolite levyne

GIACOMO DIEGO GATTA,[1,*] PAOLA COMODI,[2] PIER FRANCESCO ZANAZZI,[2] AND TIZIANA BOFFA BALLARAN[1]

[1]Bayerisches Geoinstitut, Universitaet Bayreuth, Universitaet Strasse 30, D-95447 Bayreuth, Germany
[2]Dipartimento di Scienze della Terra, Università di Perugia, Piazza Università, I-06100 Perugia, Italy

ABSTRACT

Elastic behavior and high-pressure (HP) structural evolution of a natural zeolite levyne, $(Ca_{0.5},Na,K)_6(Al_6Si_{12}O_{36})\cdot 18H_2O$, has been investigated up to 5 GPa by means of in situ single-crystal X-ray diffraction with a diamond-anvil cell using a non-penetrating pressure-transmitting medium. Peculiar elastic behavior has been observed in the range 0–1 GPa: the *c* parameter decreases between 0 and 0.2 GPa, then increases up to 0.5–0.6 GPa. Above this *P*-value, the parameter decreases as expected. Anomalous behavior is also shown by the *a*-parameter, which first increases up to 0.2 GPa, then decreases as expected. However, these anomalous lattice variations are only slightly reflected in the cell volume behavior. The low-*P* trend ($P < 1$ GPa) is also followed by the lattice parameters in decompression. The isothermal Equation-of-State (EoS) at $P > 1$ GPa, refined with a second-order Birch-Murnaghan EoS, yields the following parameters: $V_0 = 3539(3)$ Å^3 and $K_{T0} = 48(1)$ GPa. Comparison of structural refinements performed at 0.0001, 0.79(5), and 3.00(5) GPa highlights two distinct deformation mechanisms of the Si/Al-framework, one predominant at low pressures (0–1 GPa) and the other at high pressures (1–5 GPa).

The extra-framework content does not show any evident modification within the pressure range investigated.

INTRODUCTION

Levyne is an uncommon zeolite with ideal chemical formula $(Ca_{0.5},Na,K)_6(Al_6Si_{12}O_{36})\cdot 18H_2O$, found as a hydrothermal mineral in vugs in massive volcanic rocks (Gottardi and Galli 1985; Armbruster and Gunter 2001). The synthetic Si/Al/P-counterparts of levyne, SAPO-35 (Lok et al. 1984) and AlPO-35 (Zhu et al. 1997), have many technological applications as molecular sieves.

The crystal structure of levyne was first refined by Merlino et al. (1975) on the basis of the framework model previously proposed by Barrer and Kerr (1959). The framework of this zeolite can be described as a sequence of six-membered double rings and six-membered single rings (Figs. 1a and 1b), which build up the so-called "levyne-cage" and is characterized by the presence of three equivalent channel systems perpendicular to the threefold axis, confined by eight-membered rings (free diameters ~3.6 × 4.8 Å, Fig. 1b). The six-membered single ring represents the "secondary building unit" (SBU) of this framework type (SBU code: 6; Baerlocher et al. 2001). The topological symmetry is $R\bar{3}m$ and corresponds to the general symmetry of the crystal structure. The "framework density" of levyne is very low: 15.2 tetrahedra/1000 Å^3 (Baerlocher et al. 2001). The extra-framework content, represented by Ca, Na, K and water molecules, lies in the cages. At least five independent cation sites (C1, C2, C3, C4, C5, according to Merlino et al. 1975) have been located.

The crystal chemistry of levyne has been investigated by several authors (Sheppard et al. 1974; Wise and Tschernich 1976; Galli et al. 1981; Tuoto et al. 1998; Passaglia et al. 1999). Galli et al. (1981), on the basis of chemical analyses and cell parameters for 26 samples from several localities, showed an almost constant Si/(Si + Al) ratio (0.62–0.70) and a small amount of Ba and Sr present with Na, K, and Ca. An interesting remark was reported about the relationship between the amount of Na and the cell parameters: Na-rich levynes have longer *a* and shorter *c* parameters than Ca-rich levynes. The Commission of the International Mineralogical Association distinguishes between Na-levyne and Ca-levyne, defining a "levyne series" (Coombs et al. 1997). Sacerdoti (1996) provided structural refinements of several twinned samples previously studied by Galli et al. (1981). The most common morphology of levyne crystals is {001} lamellae twinned by 180° mutual rotation of two individuals around the [001] axis and with a (001) contact plane, simulating *P6*/*mmm* symmetry. Sacerdoti (1996) reported an extremely variable extra-framework content of the samples investigated, and showed that some partially occupied water molecule and cation sites are present only in some samples. On the basis of the structural data, the author reported that there is only a partial indication of tetrahedral Si-Al ordering.

The thermal behavior of a natural levyne was investigated by Gottardi and Galli (1985). The thermal curves (thermogravimetric = TG, differential thermal analysis = DTA) show water losses at 70, 180, and 300 ºC. However, no structural data on natural levynes at high-temperature are available and the dehydration mechanism is only now under investigation by means of in situ HT-single crystal diffraction at the University of Perugia, Italy.

* Present Address: Dipartimento Scienze della Terra, Universita' degli Studi di Milano, Via Botticelli 23, I-20133 Milano, ItalyE-mail: diego.gatta@unimi.it

0003-004X/05/0004–645$05.00/DOI: 10.2138/am.2005.1768

Moreover, to our knowledge, no high-pressure (HP) investigation has previously been devoted to levyne or isomorphic synthetic compounds.

The aim of the present study is to investigate the high-pressure structural behavior of natural levyne, to describe the isothermal equation-of-state and the main deformation mechanisms of the structure under pressure.

Experimental methods

The Ca-levyne specimen investigated in this study comes from Beech Creek, Grant County, Oregon. Electron microprobe analysis of a single crystal from the sample used for the X-ray diffraction study was performed with a fully automated CAMECA SX-50 microprobe, operating in WDS mode. Major and minor elements were determined with a 15 kV accelerating voltage and 10 nA beam current and a counting time of 20 s. Since this mineral loses water when heated, the crystal was mounted in epoxy resin and a defocused beam was used to minimize loss of water due to electron bombardment. The standards employed were: albite (Al, Si, Na), microcline (K), anorthite (Ca), barite (Ba), celestite (Sr), and diopside (Mg). The crystal was found to be homogeneous within analytical error. Coupled TG and DTA analysis were performed at Dipartimento di Chimica, University of Perugia with a Netzsch STA490C thermoanalyzer under a 20 mL/min air flux with a heating rate of 5 °C/min. The chemical formula, on the basis of 36 oxygen atoms, is $(Ca_{2.37}Na_{0.81}K_{0.32})_{\Sigma=3.50}(Al_{5.57}Si_{12.36})_{\Sigma=17.93}O_{36}\cdot 17.52H_2O$ ($Z = 3$). The chemical composition of this sample is close to that reported by Sheppard et al. (1974) for a Ca-levyne from the same locality (Beech Creek, Oregon); however, our sample shows slightly lower Ca content and, in contrast, slightly higher amounts of Na and K than Sheppard's sample.

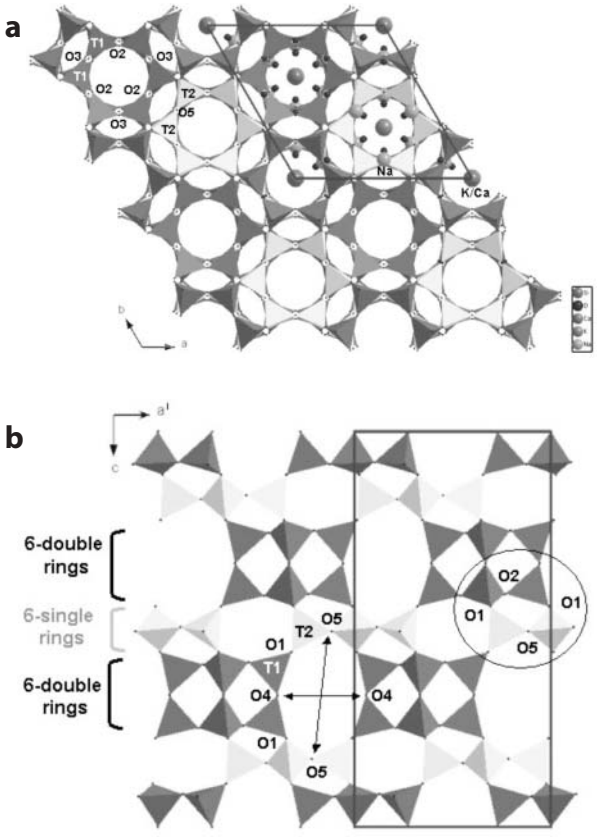

Figure 1. (**a**) Projection of the crystal structure of levyne viewed down [001], and (**b**) viewed down [010]. The [010]-channel system and the free diameters are shown. The six-single membered rings are shown in light gray, the six-double membered rings in dark gray. The "joint-unit" between six-double and six-single membered rings is highlighted (inside the circle). The extra-framework content is shown only in the view down [001]; the large spheres represent cation sites, whereas the small spheres represent the oxygen atoms of the water molecules.

As pointed out by Sacerdoti (1996), levyne crystals are often twinned (by 180° mutual rotation of two individuals around [001] and with a (001) contact plane) and it is difficult to find single-crystals free of twinning. Several crystals were tested using a polarized microscope and X-ray diffraction before finding crystals suitable for the HP experiments. The procedure proposed by Sacerdoti (1996) for checking for twinned crystals, which uses the extinction conditions (violated by twinning), was very useful.

Diffraction data were firstly collected at room conditions (crystal in air) with a Philips PW 1100 four-circle diffractometer (graphite-monochromated Mo$K\alpha$ radiation), at the Dipartimento di Scienze della Terra, University of Perugia, in the range $6° \le 2\theta \le 70°$; ω-scans with scan width = 3.0° and scan speed = 0.08°/s were used. A total of 1649 reflections were collected. Integrated intensity data (corrected for Lorentz-polarization effects) were obtained using the WinIntegr3.4 program (Angel 2003a, 2003b) and the empirical absorption correction according to North et al. (1968) was applied. A total of 1194 unique reflections with $Fo > 4\sigma(Fo)$ were employed for the structural refinement (Table 1). The crystal-structure refinement was carried out with anisotropic displacement parameters (except for the water molecules and for the partially occupied C2 and C5 sites, Table 2) in space group $R\bar{3}m$ using the SHELX-97 program (Sheldrick 1997), beginning with the atomic coordinates of Sacerdoti (1996). The hydrogen atoms were not considered; to our knowledge, they have not been localized in previous studies. Neutral atomic scattering factors, $\Delta f'$ and $\Delta f''$ coefficients from the International Tables for Crystallography (Wilson and Prince 1999) were used. The final agreement index [$R_1(F)$] was 0.084 for 74 parameters. At the end of the refinement, no peak larger than 0.9 e^-/Å was present in the final difference-Fourier synthesis. Data collection and refinement details are reported in Tables 1–2.

A three-pin Merrill-Bassett diamond anvil cell (DAC), equipped with type-I diamonds (Miletich et al. 2000) with 800 μm culet face diameter, was used for the high-pressure study in Perugia. Steel Inconel 750X foil, 250 μm thick, with a 350 μm hole, was used as the gasket material. The gasket foil was pre-indented to a thickness of 120 μm before drilling the hole. Sm^{2+}:BaFCl chips for pressure calibration, according to Comodi and Zanazzi (1993), were introduced into the DAC together with the sample. The uncertainties in the pressure measurements were ±0.05 GPa. Glycerol was used as a non-penetrating pressure-transmitting medium (Comodi et al. 2001, 2003).

The lattice parameters were determined at pressures ranging between 0.0001 and 4.27 GPa (Table 3) by least-squares refining of the UB-matrix on the basis of 80 Bragg reflections [with $I > 30\sigma(I)$]. Full-profile fit of the scanned reflections and refinement of symmetry-constrained unit-cell parameters, using the vector-least-squares method (Ralph and Finger 1982), was performed with the WinIntegr3.4 program (Angel 2003a, 2003b).

Table 1. Details of data collection and refinements of levyne at different pressures

Pressure (GPa)	0.0001	0.79(5)	3.00(5)	0.0001*
Crystal size) (μm)	160 × 180 × 80	160 × 180 × 80	160 × 180 × 80	100 × 120 × 80†
Radiation	Mo$K\alpha$	Mo$K\alpha$	Mo$K\alpha$	Mo$K\alpha$
a (Å)	13.335(2)	13.196(2)	13.000(2)	13.327(2)
c (Å)	22.823(12)	22.895(10)	22.676(10)	22.861(3)
V (Å^3)	3515(2)	3453(2)	3319(2)	3516.2(8)
θ range (°)	3–35	3–35	3–35	3–35
Scan type	ω	ω	ω	ω
Scan speed (°/s)	0.08	0.08	0.08	0.08
Scan width (°)	3.0	3.0	3.0	3.0
Space group	$R\bar{3}m$	$R\bar{3}m$	$R\bar{3}m$	$R\bar{3}m$
Reflections measured	1649	671	407	1210
Unique refl. with $F_o > 4\sigma(F_o)$	1194	201	185	882
Parameters refined	74	47	47	74
R_{int}	0.069	0.062	0.048	0.034
R_1 (F)	0.084	0.087	0.080	0.064
GooF	1.103	1.187	1.126	1.262

Note: Standard deviations are in parenthesis.
* Data collected under room conditions after the HP-experiments.
† Crystal was damaged during the opening of the DAC and the cell parameters and intensity data were measured using a fragment of the previous crystal.

HP-intensity data for the structural refinement were collected at 0.79 and 3.00 GPa in the range $6° \le 2\theta \le 70°$ with non-bisecting geometry (Denner et al. 1978). Integrated intensity data were obtained using the WinIntegr3.4 software (Angel 2003a, 2003b). Corrections for Lorentz and polarization effects were applied. Finally, diffraction data were corrected for the pressure-cell absorption with an experimental attenuation curve according to Finger and King (1978). The HP-structures were refined with isotropic atomic displacement parameters. Geometrical soft-restraints on the T-O bond distances and on O-O distances for the tetrahedra were applied. The distances between Si(Al)-O were restrained to a target value of 1.650 and 1.600 Å with an estimated standard deviation of ±0.015 Å, and the O-O distances were restrained to 2.660 ± 0.020 and 2.600 ± 0.020 Å, for the structural refinements at 0.79 and 3.00 GPa, respectively. Details of the HP-data collections and structural refinements are listed in Tables 1 and 2. Observed and calculated structure factors (Table 4) are deposited.[1]

After compression, a fragment of the crystal was recovered from the DAC and used to measure the intensities in air. These data were employed in a new refinement, to investigate possible effects of hysteresis.

A second set of HP-experiments was performed at the Bayerisches Geoinstitut (BGI), University of Bayreuth, to confirm the anomalous elastic behavior of levyne observed in Perugia and to obtain more atccurate cell parameters suitable for the elastic analysis. A single crystal (170 × 130 × 60 μm), taken from the same specimen used in Perugia, was used for the HP-experiment. A BGI-DAC, designed by Allan et al. (1996), was used for the HP study. Steel T301 foil, 250 μm thick with a 350 μm hole, was used as a gasket. The gasket foil was pre-indented to a thickness of about 110 μm before drilling the hole by spark-erosion. Glycerol was used as a non-penetrating pressure-transmitting medium. Ruby chips were used for pressure calibration, according to Mao et al. (1986). Accurate lattice parameters were determined within the pressure range between 0.0001 and 4.69 GPa (Table 3) by diffraction using a Huber four-circle diffractometer (non-monochromatized Mo$K\alpha$ radiation) with eight-position centering of 20 Bragg reflections (King and Finger 1979; Angel et al. 2000). The centering procedure and least-squares fitting of the unit-cell parameters were performed with the SINGLE99 software (Angel et al. 2000). At $P > 4.7$ GPa, a peak broadening effect was observed, with a significant increase of the FWHM. As previously reported by Gatta et al. (2004), this effect is due to the pressure medium, which becomes non-hydrostatic above 4 GPa.

TABLE 2. Refined atomic positions, site occupancy and displacement parameters (Å²) of levyne at different pressures.

Site (Whyck. pos.)	*x*	*y*	*z*	Site occupancy	U_{iso}/U_{eq}
T1 (Si,Al)	0.0002(1)	0.2323(1)	0.07008(5)	1	0.0149(3)
(36*i*)	0.0004(4)	0.2347(4)	0.0678(5)	1	0.012(1)
	0.0005(4)	0.2365(4)	0.0668(5)	1	0.013(1)
	–0.0003(11)	0.2335(1)	0.06896(5)	1	0.0160(4)
T2 (Si,Al)	0.2391(1)	0	0.5	1	0.0134(3)
(18*g*)	0.2422(5)	0	0.5	1	0.006(1)
	0.2438(4)	0	0.5	1	0.008(1)
	0.2399(1)	0	0.5	1	0.0145(4)
O1	0.0349(4)	0.3500(3)	0.1081(1)	1	0.0323(8)
(36*i*)	0.028(1)	0.348(1)	0.1085(4)	1	0.043(5)
	0.024(1)	0.346(1)	0.1092(4)	1	0.079(7)
	0.0334(4)	0.3500(4)	0.1080(1)	1	0.035(1)
O2	0.0915(3)	–0.0915(3)	0.0835(2)	1	0.028(1)
(18*h*)	0.0976(8)	–0.0975(8)	0.078(1)	1	0.041(7)
	0.1004(8)	–0.1004(8)	0.077(1)	1	0.053(7)
	0.0925(3)	–0.0925(3)	0.0816(2)	1	0.032(1)
O3	0.1288(3)	–0.1288(3)	-0.0919(2)	1	0.030(1)
(18*h*)	0.1281(7)	–0.1281(7)	-0.086(1)	1	0.033(6)
	0.1269(7)	–0.1269(7)	-0.083(1)	1	0.039(6)
	0.1285(3)	–0.1285(3)	-0.0899(3)	1	0.035(1)
O4	0.2630(5)	0	0	1	0.033(1)
(18*f*)	0.273(1)	0	0	1	0.029(6)
	0.274(1)	0	0	1	0.038(6)
	0.2687(5)	0	0	1	0.034(1)
O5	0.2225(3)	–0.2225(3)	0.1796(3)	1	0.031(1)
(18*h*)	0.2196(6)	–0.2196(6)	0.1743(9)	1	0.014(4)
	0.2182(6)	–0.2182(6)	0.1719(9)	1	0.017(4)
	0.2219(3)	–0.2219(3)	0.1783(3)	1	0.034(1)
C1 (Ca)	0	0	0.1403(1)	0.77(2)	0.023(1)
(6*c*)	0	0	0.136(2)	0.65(5)	0.026(7)
	0	0	0.134(2)	0.64(4)	0.027(7)
	0	0	0.1364(2)	0.77(1)	0.031(1)
C2 (Ca)	0	0	0.2844(8)	0.23(2)	0.059(7)
(6*c*)	0	0	0.280(3)	0.49(5)	0.04(1)
	0	0	0.276(2)	0.64(5)	0.033(8)
	0	0	0.2815(6)	0.31(3)	0.056(5)
C4 (K)	0	0	0.431(2)	0.24(2)	0.14(2)
(6*c*)	0	0	0.437(10)	0.28(6)	0.01(1)
	0	0	0.422(5)	0.28(4)	0.01(1)
	0	0	0.444(1)	0.25(2)	0.066(9)
C5 (Na)	0	0	0.5	0.3(1)	0.005(2)
(3*b*)	0	0	0.5	0.4(1)	0.08(7)
	0	0	0.5	0.5(1)	0.04(2)
	0	0	0.5	0.2(1)	0.01(1)
W1	0.1533(8)	0.0766(4)	0.2107(4)	1	0.059(2)
(18*h*)	0.152(2)	0.076(1)	0.201(2)	1	0.042(7)
	0.153(1)	0.0763(7)	0.202(2)	1	0.021(5)
	0.1528(8)	0.0764(4)	0.2093(4)	1	0.060(2)
W2	0.1218(8)	0.243(2)	0.2854(8)	1	0.159(7)
(18*h*)	0.119(1)	0.239(2)	0.285(4)	1	0.08(1)
	0.118(1)	0.237(2)	0.291(2)	1	0.048(7)
	0.1207(7)	0.241(1)	0.2866(7)	1	0.133(6)
W3	0.158(2)	0.079(1)	0.3496(8)	1	0.173(8)
(18*h*)	0.156(3)	0.078(1)	0.354(3)	1	0.07(1)
	0.158(2)	0.079(1)	0.355(3)	1	0.07(1)
	0.156(2)	0.078(1)	0.3532(8)	1	0.142(6)
W4	0.210(1)	0.421(2)	0.287(1)	0.13(1)	0.04(1)
(18*h*)	0.219(3)	0.438(6)	0.286(9)	0.13(4)	0.01(3)
	0.228(3)	0.456(7)	0.267(9)	0.12(4)	0.02(3)
	0.210(1)	0.420(2)	0.2871(1)	0.24(3)	0.028(7)

Notes: Standard deviations are in parenthesis. For each site, the values from top to bottom correspond to the refinement at 0.0001 GPa (in air), 0.79 GPa, 3.0 GPa and 0.0001 GPa (in air) after the HP-experiments. For HP-refinements the isotropic thermal parameters, U_{iso}, are reported, whereas for the room condition refinements U_{eq} are shown. C2, C5, W1, W2, W3, W4 sites were always refined as isotropic.

[1]For a copy of Table 4, document item AM-05-011, contact the Business Office of the Mineralogical Society of America (see inside front cover of recent issue) for price information. Deposit items are available on the American Mineralogist web site at http://www.minsocam.org (or contact MSA Business Office for updated link information).

TABLE 3. Lattice parameters of levyne at different pressures, measured at the University of Perugia (above) and at the Bayerisches Geoinstitut (below)

P (GPa)	*a* (Å)	*c* (Å)	*V* (Å³)
0.0001(in air)	13.335(2)	22.823(12)	3515(2)
0.0001(in the DAC)	13.336(2)	22.803(13)	3512(2)
0.10(5)	13.359(2)	22.638(8)	3499(1)
0.15(5)	13.376(2)	22.520(11)	3489(2)
0.38(5)	13.270(2)	22.801(10)	3477(2)
0.79(5)	13.196(2)	22.895(10)	3453(2)
1.72(5)	13.117(2)	22.806(11)	3398(2)
3.00(5)	13.000(2)	22.676(10)	3319(2)
3.83(5)	12.926(2)	22.589(11)	3268(2)
4.27(5)	12.894(5)	22.558(24)	3248(4)
2.88(5)*	13.001(3)	22.723(15)	3326(3)
0.05(5)*	13.359(2)	22.638(8)	3498(2)
0.52(5)†	13.246(2)	22.910(9)	3481(2)
0.0001‡	13.327(2)	22.861(3)	3516.2(8)
0.0001(in air)	13.4033(9)	22.669(2)	3526.9(7)
0.0001(in the DAC)	13.4095(9)	22.637(5)	3525.1(9)
0.16(5)	13.4144(5)	22.542(3)	3512.9(5)
0.38(5)	13.2827(9)	22.919(6)	3502.0(9)
0.54(5)	13.2543(4)	22.956(3)	3492.5(5)
1.01(5)	13.2060(4)	22.949(4)	3466.1(6)
1.22(5)	13.1866(4)	22.933(3)	3453.4(4)
1.79(5)	13.1401(4)	22.879(3)	3421.1(4)
2.61(5)	13.0698(4)	22.789(3)	3371.2(5)
3.15(5)	13.0255(5)	22.722(3)	3338.6(5)
3.83(5)	12.9751(7)	22.648(5)	3302.0(8)
4.69(5)	12.9128(9)	22.582(6)	3260.9(10)
3.12(5)*	13.0259(5)	22.727(5)	3339.6(7)
0.91(5)*	13.2167(5)	22.953(7)	3472.3(8)

Note: Standard deviations are in parentheses.
* Data collected during decompression.
† Data collected during further compression (re-compression).
‡ Final data collected in air.

RESULTS

Crystal structure at room conditions

The crystal structure of levyne was first refined at room pressure, with the crystal in air, starting with the atomic coordinates reported by Sacerdoti (1996). The refined coordinates of the framework and extra-framework sites (Table 2) are close to those found by Merlino et al. (1975) and Sacerdoti (1996). The main differences were found in the extra-framework content, as expected for a sample with different composition.

On the basis of the electronic density and bond distances, we consider that the C1 and C2 sites are occupied by Ca (~77% and ~23%, respectively). The C4 site is occupied by K (~24%) and the C5 site by Na (~30%). The C3 site, reported by Merlino et al. (1975) and Sacerdoti (1996) to be partially occupied by Na, is completely empty in our sample. In agreement with Merlino et al. (1975), we found four water sites (W1, W2, W3, W4) with variable occupancy. In contrast, Sacerdoti (1996) found samples of levyne with three supplementary water sites (W5, W6, W7), characterized by low occupancies (17–34%). The occupancies of the cations sites were not constrained during the refinement and our results show a good agreement with the chemical analysis of the same sample. Determination of the Al content of the tetrahedra was carried out using the methods proposed by Jones (1968). Starting from the structural data from the crystal at 0.0001 GPa (in air), we obtained: T1(Al) = 33.6%, T2(Al) = 18.8%, with a total Al content equal to 5.16 afu. (5.57 afu. by chemical analysis). As expected, the Jones method underestimates the Al content, in particular for microporous framework silicates (Alberti and Gottardi 1988; Comodi et al. 2001; Gatta et al. 2004). However, we can support the previous results of Sacerdoti (1996), who reported that the distribution of Al in the tetrahedra is somewhat ordered: T1(Al) = 35% and T2(Al) = 25%. The T1-O and T2-O bond distances are reported in Table 5.

H*P*-elastic behavior

Figure 2 shows the evolution of the lattice parameters of levyne with pressure from two independent data sets collected at the University of Perugia and at the Bayerishes Geoinstitut, respectively. A peculiar elastic behavior is observed in the range 0–1 GPa: the *c* parameter decreases between 0 and 0.2 GPa, then increases up to 0.8 GPa (Fig. 2, Table 3). Above this pressure the parameter decreases as expected. An anomalous behavior is also shown by the *a* parameter, which first increases up to 0.2 GPa,

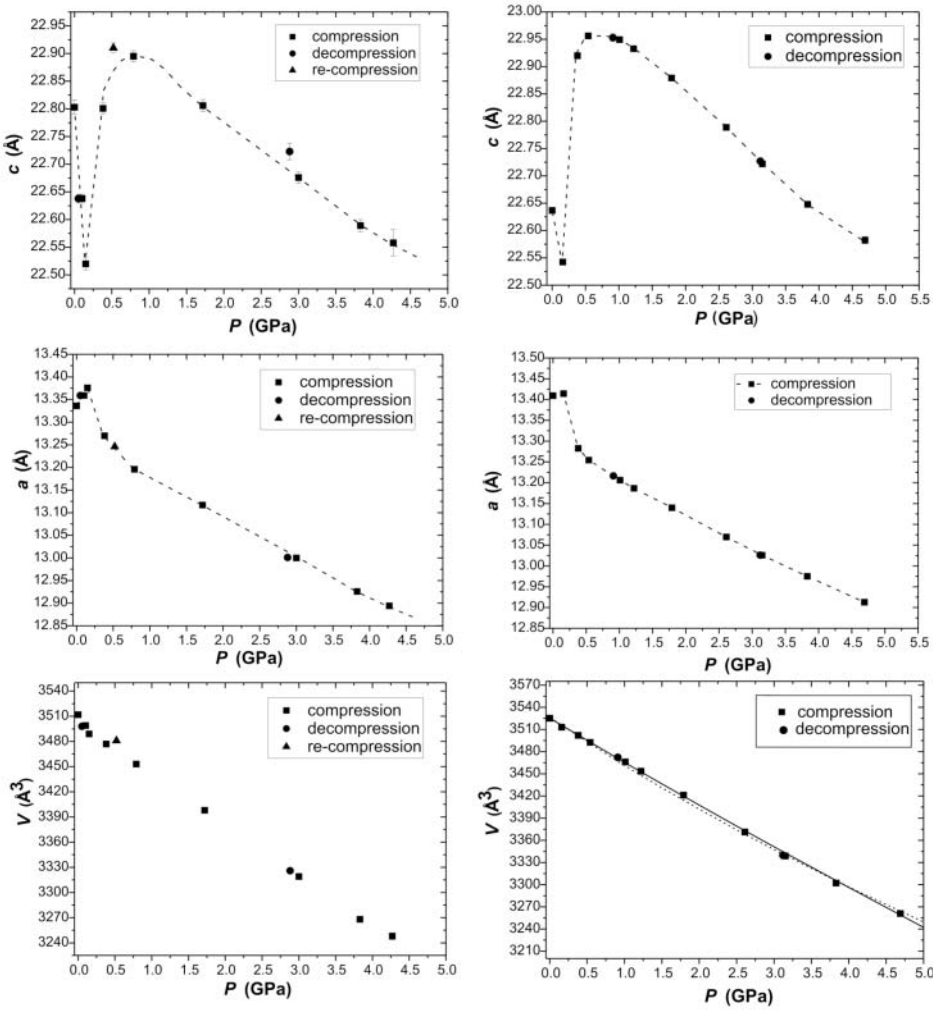

FIGURE 2. Evolution of the unit-cell parameters of levyne as a function of pressure. Data measured at the University of Perugia (left side) and at the Bayerisches Geoinstitut (BGI) (right side). Dashed lines for the *a* and *c*-axis diagrams are added as "guide to the eyes." For the volume data from BGI, the solid line represents the III-BMEoS-fit with all the volume data ($0.0001 < P < 5$ GPa), whereas the dotted line represents the II-BMEoS-fit in the same pressure range (see text).

TABLE 5. Selected interatomic distances (Å) as a function of pressure

P (GPa)	0.0001	0.79	3.00	0.0001*
T1-O1	1.644(3)	1.64(1)	1.62(1)	1.648(8)
T1-O4	1.651(2)	1.634(9)	1.593(9)	1.645(2)
T1-O3	1.655(2)	1.629(8)	1.597(7)	1.650(2)
T1-O2	1.676(2)	1.627(8)	1.600(7)	1.679(3)
<T1-O>	1.656	1.632	1.602	1.655
T2-O1 (×2)	1.633(4)	1.626(7)	1.600(7)	1.631(4)
T2-O5 (×2)	1.634(2)	1.617(5)	1.596(4)	1.633(2)
<T2-O>	1.633	1.621	1.598	1.632
C1-W1 (×3)	2.390(9)	2.29(5)	2.31(5)	2.426(9)
C1-O2 (×3)	2.478(6)	2.60(3)	2.61(3)	2.476(7)
C1-O3 (×3)	3.176(7)	3.14(3)	3.09(3)	3.151(6)
C2-W3 (×3)	2.36(2)	2.45(8)	2.52(6)	2.44(2)
C2-W1 (×3)	2.44(2)	2.51(7)	2.40(5)	2.41(1)
C2-W2 (×3)	2.81(2)	2.74(3)	2.69(3)	2.79(2)
C4-W3 (×3)	2.61(4)	2.6(2)	2.35(9)	2.76(3)
C4-O5 (×3)	2.86(3)	2.9(1)	3.07(7)	2.76(1)
C4-W4 (×3)	3.07(4)	2.9(2)	2.4(1)	3.20(2)
C5-O5(×6)	2.577(6)	2.60(1)	2.59(1)	2.585(7)
C4-C5	1.57(5)	1.4(2)	1.8(1)	1.27(3)

Note: Standard deviations are in parenthesis.
* Data collected at room condition after the HP-experiments.

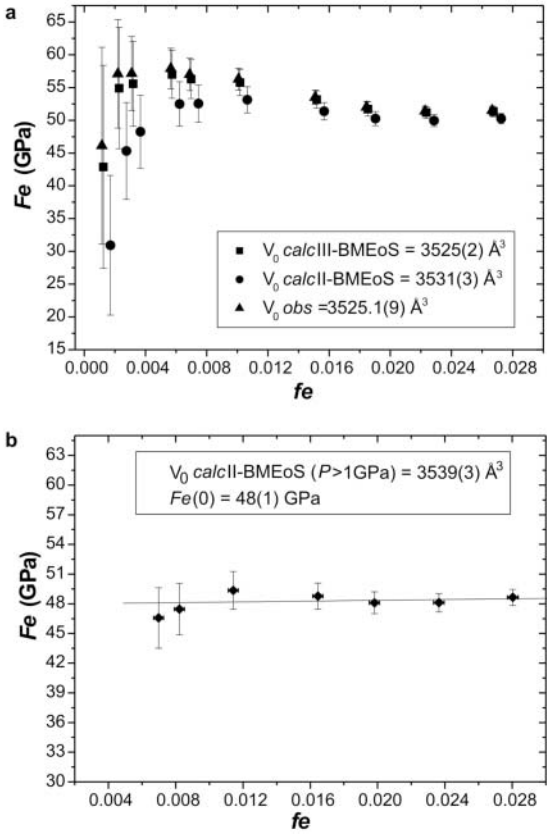

FIGURE 3. Plot of the volume finite strain $f_e = [(V_0/V)^{2/3} - 1]/2$ vs. the "normalized stress," defined as $F_e = P/[3f(1+2f)^{5/2}]$, for levyne in glycerol. (**a**) *fe-Fe* plot calculated using the measured *V*-values within the range $0.0001 < P < 5$ GPa, adopting the observed V_0-value (triangles) and the calculated V_0-values with a II- and III-BMEoS, respectively (circles, squares); (**b**) *fe-Fe* plot calculated using only the *V*-data at $P > 1$ GPa, using the V_0-value calculated with a II-BMEoS at $P > 1$ GPa (see text). In the latter case, the regression lines through the data points is shown and the calculated *Fe*(0) is reported. The e.s.d.s were calculated according to Heinz and Jeanloz (1984).

then decreases. However, the combined effect of these lattice variations results in a decrease of the cell volume.

We performed the elastic analysis of the compressional behavior of levyne using the accurate volume data measured at the BGI between 0.0001 and 5 GPa. The eulerian strain vs. normalized pressure plot (*fe-Fe* plot, Angel 2000) is shown in Figure 3a. At low pressure, a change in slope is clearly visible. Since the *fe-Fe* plot is strongly influenced by the uncertainty in V_0 (Angel 2000; Angel and Jackson 2002), two supplementary sets of finite strain-stress data were calculated adopting the V_0 value obtained by fitting all volume data (without the experimental V_0) with a second-order and third-order Birch-Murnaghan Equation of State (II-, III-BMEoS) (Birch 1947), respectively. The EoS-fit was obtained with the EOS-FIT5.2 program (Angel 2001) using the data weighted by the uncertainties in *P* and *V*. The resulting EoS refined parameters are: $V_0 = 3525(2)$ Å^3, $K_{T0} = 57(2)$ GPa, and $K' = 1.0(9)$, for III-BMEoS; $V_0 = 3531(3)$ Å^3, $K_{T0} = 50(1)$ GPa, for II-BMEoS. Although there is a slight difference between the V_0 value obtained using II-BMEoS with respect to the experimental value and that obtained using III-BMEoS, the corresponding *fe-Fe* plots show a similar change in slope at low pressure (Fig. 3a). Moreover, both II- and III-BMEoS fits show a small discrepancy with respect to the experimental data at $P >$ 1.5 GPa (Fig. 2). It appears, therefore, that the elastic behavior of levyne is better described by two different equations of state, one for $P < 1$ GPa and one for $P > 1$ GPa.

A further *fe-Fe* plot was obtained using only the volume data between 1 and 5 GPa and the V_0 value from the II-BMEoS for these data (Fig. 3b). The EoS refined parameters with the volume data measured between 1 and 5 GPa are: $V_0 = 3539(3)$ Å^3 and $K_{T0} = 48(1)$ GPa for II-BMEoS; $V_0 = 3537(7)$ Å^3, $K_{T0} = 49(5)$ GPa, and $K' = 3(2)$ for III-BMEoS. The weighted linear regression through the data point of the *fe-Fe* plot yields Fe(0) = 48(1) GPa, in excellent agreement with the K_{T0} value previously obtained with the II-BMEoS fit. The almost horizontal weighted linear regression justifies the use of a second-order BM-EoS for fitting the volume data within the 1–5 GPa range (Fig. 3b). The elastic behavior at $P < 1$ GPa is described by means of the resulting II-BMEoS parameters: $V_0 = 3524(1)$ Å^3 and $K_{T0} = 56(4)$ GPa. The II-BMEoS fits at $P < 1$ GPa and at $1 < P < 5$ GPa are shown in Figure 4.

The axial anisotropy of levyne has been calculated as the ratio between the linearized bulk moduli along *a* and *c* at $P > 1$ GPa. A "linearized BM-EoS" (Angel 2000), truncated to the second-order, yields the following axial parameters: $a_0 = 13.305(4)$ Å and $K_{T0}(a) = 43.7(8)$ GPa; $c_0 = 23.079(8)$ Å and $K_{T0}(c) = 62(1)$ GPa. Thus, the lattice shows a strong anisotropy, being more compressible along a than along c with $K_{T0}(a):K_{T0}(c) = 1.00:1.42$.

Unit-cell parameters measured during decompression (Fig. 2, Table 3) show that the lattice is basically restored. A supplementary data point was collected in Perugia under further compression ("re-compression") at 0.52 GPa, and showed that the low-*P* elastic behavior is reversible, without any evident hysteresis effect. The cell constants measured in Perugia for the crystal in air after the end of the HP-experiments reported a cell volume equal (within error) to the value previously measured before the HP experiments.

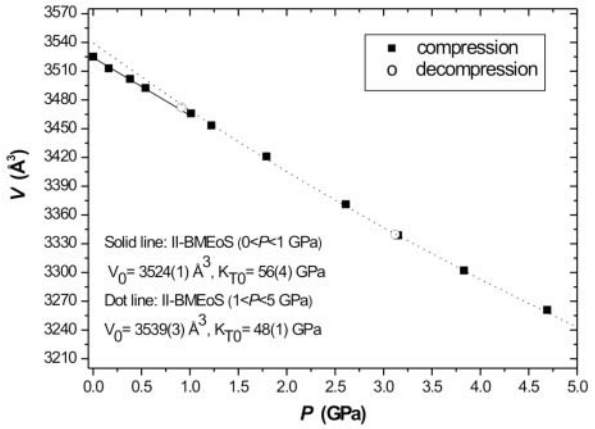

FIGURE 4. II-BMEoS fit at $P < 1$ GPa (solid line) and at $1 < P < 5$ GPa (dotted line) of levyne in glycerol.

H*P* structural evolution

Four structural refinements were carried out at 0.0001 (with crystal in air), 0.79, 3.00, and 0.0001 GPa (in air, after the HP experiments) to understand the structural evolution of this zeolite at high pressure.

Tetrahedral bond distances (Table 5) appear to be slightly affected by the pressure increase: <T1-O> changes from 1.656 Å under room conditions to 1.602 Å at 3.00 GPa; <T2-O> varies from 1.633 Å to 1.598 Å in the same pressure range. However, as pointed out in the previous studies on the HP-behavior of microporous framework-silicates (Hazen and Finger 1979; Gatta et al. 2003; Gatta and Wells 2004) the main deformation mechanisms are basically related to the polyhedral tilting, which results in inter-tetrahedral angle variations. In this case, analysis of the tetrahedral tilting is the key to understanding the anomalous elastic behavior of levyne. At $P < 1$ GPa the *P*-induced tetrahedral tilting gives rise to an increase in the O1-O4-O1 angle and in the O1-O1 distance of the six-membered double ring (Fig. 5, Table 6). This mechanism is responsible for the [001]-elongation of the crystal lattice. At about 1 GPa the six-double ring achieves a geometrical configuration that cannot allow further expansion along [001]. It is clear, therefore, that the unexpected increase of the *c* parameter at $P < 1$ GPa is due to the tetrahedral tilting of the six-membered double rings. Due to the tetrahedral tilting, the ditrigonal rings become pseudo-hexagonal at 0.79 GPa, although at higher pressure ($P = 3.00$ GPa) the structural refinement shows a new ditrigonal distortion (see the T1-O4-T1 and T1-O2-T1 angle values in Table 6). It appears, therefore, that at 0.79 GPa the lattice is very close to hexagonal symmetry, but on further compression becomes more trigonally distorted. At $P > 1$ GPa, the well-packed six-double rings behave like rigid-units and the main deformation mechanism is the tetrahedral tilting which modifies the bridges among (six-*double* rings)-(six-*single* ring)-(six-*double* rings) (Fig. 1b). In fact, the six-membered single ring can be considered as a "joint" between the six-double rings. In particular, the O1-O1 distance (of the joint unit) increases and the O2-O5 distance decreases with pressure (Fig. 1b, Table 6); at the same time, the O2-O1-O5 angle decreases whereas the O1-O5-O1 angle increases at high pressure (Fig. 1b, Table 6). As shown in Table 6, this mechanism also occurs at lower pressure ($P < 1$ GPa), but in such a *P*-range the tilting behavior of the six-double rings is predominant. The main deformation mechanism at $P > 1$ GPa gives rise to the expected elastic behavior: all the cell parameters show a *P*-induced shortening up to the maximum pressure achieved.

We also analyzed the modification of the [100]-channel ellipticity as a consequence of the applied pressure. The ellipticity, $\varepsilon_{[100]}$, is defined here as the ratio between the smaller "free diameter" (↔, the distance between the oxygen sites, less twice the radius of an oxygen atom, which we take to be 1.35

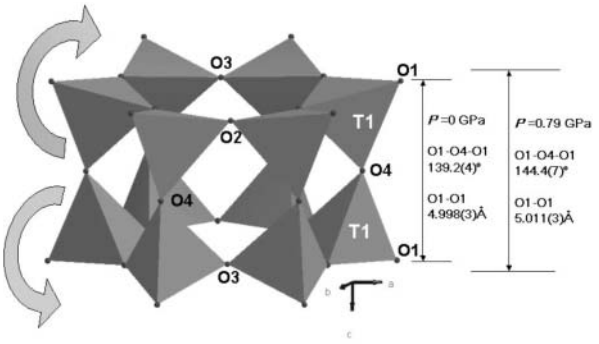

FIGURE 5. The main deformation mechanism of the crystal structure of levyne at $P < 1$ GPa.

TABLE 6. Selected structural parameters of levyne at different pressures.

P (GPa)	0.0001	0.79(5)	3.00(5)	0.0001*
[001] 6-membered double ring				
T1-O4-T1(°)	151.2(3)	143.4(4)	143.8(8)	146.9(5)
T1-O2-T1(°)	134.5(2)	143.4(6)	146.0(6)	135.9(5)
T1-O3-T1(°)	139.0(2)	144.5(6)	149.5(8)	141.1(6)
O2-O3 (Å) (on the (001)-plane)	5.097(3)	5.162(4)	5.122(5)	5.104(4)
O1-O1 (Å)	4.998(3)	5.011(3)	4.985(6)	5.000(3)
O2-O4-O3(°)	96.6(2)	90.9(2)	89.4(5)	93.8(2)
O4-O3-O4(°)	79.7(2)	84.4(4)	86.5(6)	82.0(2)
O1-O4-O1(°)	139.2(4)	144.4(7)	145.4(9)	142.0(5)
[001] 12-membered ring				
O5-O3 (Å)	9.965(3)	9.851(3)	9.724(6)	9.963(4)
O5↔O3 ("free diameter") (Å)	7.264(3)	7.151(3)	7.024(6)	7.263(4)
O1-O1 (Å)	9.598(2)	9.347(4)	9.131(7)	9.552(2)
O1↔O1 (Å)	6.898(2)	6.647(4)	6.431(7)	6.852(2)
$O1\text{-}O1_{(short)}$ (Å)	8.871(2)	8.808(3)	8.687(6)	8.884(2)
$O1\leftrightarrow O1_{(short)}$ (Å)	6.171(2)	6.108(3)	5.987(6)	6.184(2)
[100] 8-membered ring channel				
O5-O5 (Å)	7.477(4)	7.674(2)	7.679(5)	7.534(2)
O5↔O5 (Å)	4.777(4)	4.974(2)	4.979(5)	4.834(2)
O4-O4 (Å)	6.320(2)	5.980(2)	5.867(4)	6.164(2)
O4↔O4 (Å)	3.620(2)	3.280(2)	3.167(4)	3.464(2)
O1-O1 (Å)	6.701(3)	6.660(3)	6.591(4)	6.689(2)
O1↔O1 (Å)	4.001(3)	3.960(3)	3.891(4)	3.989(2)
$\varepsilon_{[100]}$ †	0.76	0.66	0.64	0.72
O1-O5-O1(°)	117.0(3)	112.7(4)	111.2(7)	115.8(3)
O1-O4-O1(°) (see above)				
"Joint-unit"				
O2-O1-O5(°)	86.4(2)	83.3(3)	81.2(3)	85.9(2)
O1-O5-O1(°)	87.1(2)	92.8(3)	95.9(4)	88.5(3)
O1-O2-O1(°)	85.8(2)	91.4(6)	94.4(4)	86.7(2)
O2-O5 (Å)	3.737(2)	3.555(4)	3.411(3)	3.718(2)
O1-O1(Å)	3.738(2)	3.849(3)	3.869(5)	3.775(2)

Notes: $\varepsilon_{[100]}$ = O4↔O4/O5↔O5 (see text). Standard deviations are in parentheses.
* Data collected at room condition after the HP-experiments
† e.s.d. values are less than 0.008

Å, according to Baerlocher et al. 2001) and the larger one. Thus $\varepsilon_{[100]}$ = O4 ↔ O4/O5 ↔ O5, for the distorted eight-membered ring channel along [100]. $\varepsilon_{[100]}$ is 0.76 at room pressure, 0.66 at 0.79 GPa and 0.64 at 3.00 GPa (Table 6). In other words, the ellipticity of the [100]-channels increases rapidly at low pressure (about +13% between 0.0001 and 0.79 GPa) and at $P > 1$ GPa is practically constant (about +3% between 0.79 and 3.00 GPa). This increase at $P < 1$ GPa is correlated with elongation of the *c* parameter at low pressure (Fig. 1b).

The extra-framework content does not show relevant modifications under pressure conditions and the topological configuration of the polyhedra is maintained (Tables 2 and 5). A slight distortion of the polyhedra, rather than a relevant reduction of the average bond distances, is observed with increasing pressure, as well as an expected decrease of the displacement parameters (except for the partially occupied C5 site, Table 2). The occupancy factor of the C2 site increases slightly with pressure (Table 2). We cannot exclude, however, that this is an artifact due to the quality of the HP structural refinements. A less probable explanation can be given by the slight decrease of the C1 site occupancy with pressure, which may suggests a *P*-induced ordering. In addition, the change in C5 occupancy with *P* and the relative high e.s.d. could be due to the difficultly of detecting of light elements (i.e., Na with a low site occupancy), one of the limitations of HP-crystallography.

Discussion

Levyne is the first natural zeolite belonging to the "zeolites with six-membered rings" group (Gottardi and Galli 1985; Armbruster and Gunter 2001) investigated under pressure conditions. The lattice evolution with pressure is characterized by an anomalous elastic behavior at $P < 1$ GPa (Fig. 2, Table 3). The analysis of the elastic behavior performed by fitting the volume data under pressure with a BM-EoS, and by the *fe-Fe* plot, shows that there is a change in compression mechanism at $P > 1$ GPa. This change leaves the crystal structure iso-symmetric. In fact, the data collection performed for the structure refinement shows that space group $R\bar{3}m$ is maintained within the investigated pressure range without violation. On the basis of the lattice parameter variations and of the structure refinements, we expect that such compressional change is "reversible". The structure refinement of the crystal in air after the HP experiments shows that the framework and extra-framework configuration is essentially restored at room condition after decompression (Tables 2, 5, and 6). In particular, the six-membered double ring shows a configuration similar to the previous one on the (001)-plane (i.e., T1-O2-T1 < T1-O3-T1, Table 6). The O1-O4-O1 angle appears to preserve a residual HP arrangement, the distance of the "joint-unit" O1-O1 is slightly higher, and O2-O5 is slightly lower than the co-respective values measured before the compression experiment (Fig. 1b, Table 6). However, the cell volume is similar to the initial volume measured before compression (Table 1). We cannot exclude the possibility that slight differences observed in the crystal structure at room conditions, after and before the HP experiments, could be due to the fact that the crystal was damaged during the opening of the DAC and the cell parameters and intensity data were measured after the HP experiments using a fragment of the previous crystal (Table 1).

As observed for other microporous framework silicates, tetrahedral tilting basically drives the *P*-induced structural transformations. Such a mechanism may induce "displacive" phase transitions (i.e., for analcime, Hazen and Finger 1979) or a continuous rearrangement of the framework without any phase transitions. The latter case is more common for zeolites (Comodi et al. 2001, 2002, 2003; Gatta et al. 2004; Lee et al. 2004) when a non-penetrating pressure medium is used. For levyne, the main deformation mechanism at low *P* is represented by the cooperative rotation of the tetrahedra belonging to the six-membered double rings. The cooperative anti-rotation mechanism of the T1 tetrahedra around the O4 hinge gives rise to elongation of the *c* dimension (Fig. 5). This behavior is in agreement with the model proposed by Baur (1992) and Baur et al. (1996), and highlighted by Ross (2000) and Gatta et al. (2003), for the "non-collapsibility" of zeolite and feldspar frameworks (at different *P-T-X* conditions) due to a self-regulating mechanism based on anti-rotation of the hinges (i.e., bridging oxygen atoms). Such anti-rotation simultaneously induces "compression" and "extension" inside the framework, because the compression at one hinge necessitates expansion at another hinge. At $P >$ 1 GPa, levyne shows an expected elastic behavior: all the cell parameters decrease with pressure. In fact, the anti-rotation mechanism previously described cannot continue because the six-double rings achieve a stable/limit configuration and behave like rigid units. Then, the effect of pressure is accommodated by the bridges among (six-*double* rings)-(six-*single* ring)-(six-*double* rings) ("joint-unit", Fig. 1b, Table 6) and by a slight *P*-induced reduction of the T-O bond distances (Table 5). The anisotropic compressibility of levyne at $P > 1$ GPa is basically due to the tetrahedral framework evolution: because the rigid six-double and six-single rings are parallel to [001], there is a smaller compressibility along **c** than along **a**.

The behavior of the extra-framework content with pressure does not show relevant modifications: the topological configuration and the coordination number of the polyhedra is maintained and a general expected decrease of the displacement parameters is observed (Table 2). The high e.s.d.s values do not permit an extensive discussion on the modification of the bond distances, however a slight *P*-induced distortion of some polyhedra can be observed (Table 5). As pointed out by Gatta et al. (2003, 2004), this study confirms that the elastic behavior of zeolites is basically driven by the framework response under pressure and the role of the extra-framework content appears to be secondary.

Acknowledgments

We thank R. Vivani (University of Perugia) for the thermogravimetric analysis of the levyne sample. We also thank the Associate Editor A. Pawley, M. Gunter, and an anonymous referee for their helpful suggestions. This work was financially supported by the Italian M.U.R.S.T grant to P.F. Zanazzi and by the Sofia Kovalevskaja Award to T. Boffa Ballaran. Structural visualization was performed with the DIAMOND program (Pennington 1999).

References cited

Alberti, A. and Gottardi, G. (1988) The determination of Al-content in the tetrahedra of framework silicates. Zeitschrift für Kristallographie, 184, 49–61.

Allan, D.R., Miletich, R., and Angel, R.J. (1996) A diamond-anvil cell for single-crystal X-ray diffraction studies to pressures in excess of 10 GPa. Review of Scientific Instruments, 67, 840–842.

Angel, R.J. (2000) Equation of State. In R.M. Hazen and R.T. Downs, Eds., High-Temperature and High-Pressure Crystal Chemistry. Reviews in Mineralogy and Geochemistry, 41, 35–59. Mineralogical Society of America,

Washington, D.C.
——— (2001) EOS-FIT V6.0. Computer program. Crystallography Laboratory, Department of Geological Sciences, Virginia Tech, Blacksburg.
——— (2003a) Automated profile analysis for single-crystal diffraction data. Journal of Applied Crystallography, 36, 295–300.
——— (2003b) WIN-INTEGRSTP V3.4. Computer program. Crystallography Laboratory, Department Geological Sciences, Virginia Tech, Blacksburg.
Angel, R.J. and Jackson, J.M. (2002) Elasticity and equation of state of orthoenstatite, $MgSiO_3$. American Mineralogist, 87, 558–561.
Angel, R.J., Downs, R.T., and Finger, L.W. (2000) High-temperature–high-pressure diffractometry. In R.M. Hazen and R.T. Downs, Eds., High-Temperature and High-Pressure Crystal Chemistry, 41, 559–596. Reviews in Mineralogy and Geochemistry, Mineralogical Society of America, Washington, D.C.
Armbruster, T. and Gunter, M.E. (2001) Crystal structures of natural zeolites. In D.L. Bish and D.W. Ming, Eds., Natural zeolites: occurrence, properties, application, 45, 1–57. Reviews in Mineralogy and Geochemistry, Mineralogical Society of America, Washington, D.C.
Baerlocher, Ch., Meier, W.M., and Olson, D.H. (2001) Atlas of zeolite framework types, 5th ed., 302 p. Elsevier, Amsterdam.
Barrer, R.M. and Kerr, I.S. (1959) Intracrystalline channels in levynite and some related zeolites. Transactions of the Faraday Society, 55, 1915–1923.
Baur, W.H. (1992) Self-limiting distortion by anti-rotation hinges is the principle of flexible but noncollapsable framework. Journal of Solid State Chemistry, 97, 243–247.
Baur, W.H., Joswig, W., and Müller, G (1996) Mechanisms of the feldspar framework: crystal structure of Li-feldspar. Journal of Solid State Chemistry, 12, 12–23.
Birch, F. (1947) Finite elastic strain of cubic crystal. Physical Review, 71, 809–824.
Comodi, P. and Zanazzi, P.F. (1993) Improved calibration curve for the Sm^{2+}: BaFCl pressure sensor. Journal of Applied Crystallography, 26, 843–845.
Comodi, P., Gatta, G.D., and Zanazzi, P.F. (2001) High-pressure structural behavior of heulandite. European Journal of Mineralogy, 13, 497–505.
——— (2002) High-pressure behavior of scolecite. European Journal of Mineralogy, 14, 567–574.
——— (2003) Effects of pressure on the structure of bikitaite. European Journal of Mineralogy, 15, 247–225.
Coombs, D.S., Alberti, A., Armbruster, T., Artioli, G., Colella, C., Galli, E., Grice, J.D., Liebau, F., Mandarino, J.A., Minato, H., Nickel, E.H., Passaglia, E., Peacor, D.R., Quartieri, S., Rinaldi, R., Ross, M., Sheppard, R.A., Tillmanns, E., and Vezzalini, G. (1997) Recommended nomenclature for zeolite minerals: report of the Subcommittee on Zeolites of International Mineralogical Association, Commission on new minerals and minerals names. Canadian Mineralogist, 35, 1571–1606.
Denner, W., Schulz, H., and d'Amour, H. (1978): A new measuring procedure for data collection with high-pressure cell on X-ray four-circle diffractometer. Journal of Applied Crystallography, 11, 260–264.
Finger, L.W. and King, H. (1978): A revised method of operation of the single-crystal diamond cell and refinement of the structure of NaCl at 32 kbar. American Mineralogist, 63, 337–342.
Galli, E., Rinaldi, R., and Modena, C. (1981) Crystal chemistry of levyne. Zeolites, 1, 157–160.
Gatta, G.D. and Wells, S.A. (2004) Rigid Unit Modes at high-pressure: an explorative study of a fibrous zeolite like framework with EDI topology. Physics and Chemistry of Minerals, 31, 465–474.
Gatta, G.D., Comodi, P., and Zanazzi, P.F. (2003) New insights on high-pressure behavior of microporous materials from X-ray single-crystal data. Microporous and Mesoporous Materials, 61, 105–115.
Gatta, G.D., Boffa Ballaran, T., Comodi, P., and Zanazzi, P.F. (2004) Isothermal equation of state and compressional behavior of tetragonal edingtonite. American Mineralogist, 89, 633–639.
Gottardi, G. and Galli, E. (1985) Natural Zeolites, 409 p. Springer-Verlag, Berlin.
Hazen, R.M. and Finger, L.W. (1979) Polyhedral tilting: a common type of pure displacive phase transition and its relationship to analcite at high pressure. Phase Transitions, 1, 1–22.
Heinz, D.L. and Jeanloz, R. (1984) The equation of state of the gold calibration standard. Journal of Applied Physics, 55, 885–893.
Jones, J.B. (1968) Al-O and Si-O tetrahedral distances in aluminosilicate framework structures. Acta Crystallographica, B24, 355–358.
King, H.E. and Finger, L.W. (1979) Diffracted beam crystal centering and its application to high-pressure crystallography. Journal of Applied Crystallography, 12, 374–378.
Lee, Y., Hriljac, J.A., Studer, A., and Vogt, T. (2004) Anisotropic compression of edingtonite and thomsonite to 6 GPa at room temperature. Physics and Chemistry of Minerals, 31, 22–27.
Lok, B.M., Messina, C.A., Patton, R.L., Gajek, R.T., Cannan, T.R., and Flanigen, E.M. (1984) Silicoaluminophosphate molecular sieves: another new class of microporous crystalline inorganic solids. Journal of the American Chemical Society, 106, 6092–6093.
Mao, H.K., Xu, J., and Bell, P.M. (1986) Calibration of the ruby pressure gauge to 800 kbar under quasi-hydrostatic conditions. Journal of Geophysical Research, 91, 4673–4676.
Merlino, S., Galli, E., and Alberti, A. (1975) The crystal structure of levyne. Tschermaks Mineralogische und Petrographische Mitteilungen, 22, 117–129
Miletich, R., Allan, D.R., and Kush, W.F. (2000) High-pressure Single-Crystal Techniques. In R.M. Hazen and R.T. Downs, Eds., High-Temperature and High-Pressure Crystal Chemistry, 41, 445–519. Reviews in Mineralogy and Geochemistry, Mineralogical Society of America, Washington, D.C.
North, A.C.T., Phillips, D.C., and Mathews, F.S. (1968): A semiempirical method of absorption correction. Acta Crystallographica, A24, 351–359.
Passaglia, E., Marchi, E., and Gualtieri, A.F. (1999) Chemistry of levynes and epitaxially overgrown erionites. Neues Jahrbuch für Mineralogie Monatshefte, 1999(12), 568–576.
Pennington, W.T. (1999) DIAMOND-Visual Crystal Software Information System. Journal of Applied Crystallography, 32, 1028–1029.
Ralph, R.L. and Finger, L.W. (1982) A computer program for refinement of crystal orientation matrix and lattice constants from diffractometer data with lattice symmetry constraints. Journal of Applied Crystallography, 15, 537–539.
Ross, N.L. (2000) Framework Structures. In R.M. Hazen and R.T. Downs, Eds., High-Temperature and High-Pressure Crystal Chemistry, 41, 257–287. Reviews in Mineralogy and Geochemistry, Mineralogical Society of America, Washington, D.C.
Sacerdoti, M. (1996) New refinements of the crystal structure of levyne using twinned crystals. Neues Jahrbuch für Mineralogie Monatshefte, 3, 114–124.
Sheldrick, G.M. (1997) SHELX-97. Programs for crystal structure determination and refinement. University of Göttingen, D.
Sheppard, R.A., Gude A.J., Desborough, A., and White, J.S. (1974) Levyne-offretite intergrowths from basalt near Beech Creek, Grant County, Oregon. American Mineralogist, 59, 837–842.
Tuoto, C.V., Regina, A., Nagy, J.B., and Nastro, A. (1998) Influence of the SiO_2/Al_2O_3 ratio on the synthesis and physicochemical characteristics of levyne-type zeolite. Microporous and Mesoporous Materials, 20, 247–257.
Wilson, A.J.C. and Prince, E., Eds. (1999) International Tables for X-ray Crystallography, Volume C: Mathematical, physical and chemical tables (2nd Edition). Kluwer Academic, Dordrecht.
Wise, W.S. and Tschernich, R.W. (1976) Chemical compositions and origin of zeolites offretite, erionite, and levyne. American Mineralogist, 61, 853–863.
Zhu, G.S., Xiao, F.S., Qiu, S.L., Hun, P.C., Xu, R.R., Ma, S.J., and Terasaki, O. (1997) Synthesis and characterization of a new microporous aluminophosphate with levyne structure in the presence of HF. Microporous Materials, 11, 269–273.

MANUSCRIPT RECEIVED JULY 16, 2004
MANUSCRIPT ACCEPTED OCTOBER 19, 2004
MANUSCRIPT HANDLED BY ALISON PAWLEY